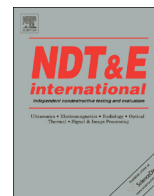




ELSEVIER

Contents lists available at ScienceDirect

NDT&amp;E International

journal homepage: [www.elsevier.com/locate/ndteint](http://www.elsevier.com/locate/ndteint)

# Dynamic thermal tomography: Recent improvements and applications



Vladimir P. Vavilov\*

Tomsk Polytechnic University, Savinykh Street, 7, 634028, Russia

## ARTICLE INFO

### Article history:

Received 23 June 2014

Received in revised form

2 September 2014

Accepted 17 September 2014

Available online 12 January 2015

### Keywords:

Thermal/infrared non-destructive testing

Infrared thermography

Dynamic thermal tomography

Numerical models

Carbon fiber reinforced plastic

## ABSTRACT

The concept of “dynamic thermal tomography” (DTT) was suggested in the 1980s. At that time, there was a wave of interest in the tomographic analysis of materials by active thermal nondestructive testing (TNDT). Unlike particles and quanta of electromagnetic radiation, thermal energy propagates in solids by diffusion. Therefore, a purely geometrical approach, that is characteristic of computed X-ray tomography, is replaced in DTT with the analysis of the evolution of temperature *versus* time. DTT is based on the fact that, in one-sided TNDT, deeper material layers are characterized by longer time delays of the thermal response. The DTT algorithm is relatively stable when used in the inspection of certain materials. Thermal waves experience damping by amplitude and retardation in time. This limits the detection depth and produces certain artifacts that can be suppressed by thresholding maxigrams. DTT can also be considered as a specific way of data presentation that has proven to be useful in many practical cases, including surface and volumetric thermal stimulation of both metals and non-metals. Thermal tomograms appear similar to binary maps of defects, thus enabling more reliable defect detection in comparison to conventional IR thermograms. In this paper, a “reference-free” approach to DTT is proposed being based on some mathematical manipulations with a front-surface temperature response. Also, the possibility of using the DTT principles for processing the results of ultrasonic infrared thermography is demonstrated.

© 2015 Elsevier Ltd. All rights reserved.

## 1. Introduction

One may combine the terms “tomography” with “infrared,” “thermographic” and “thermal” to describe a number of different techniques used for reconstructing the internal structure of opaque solids. Emission IR thermographic tomography of semi-transparent gases and plasma [1,2], as well as IR tomography of charge carriers in semiconductors [3], is the technique that is closest to the classical computed tomography which utilizes a principle of ray-like propagation of electromagnetic radiation and/or charged particles. The temperature inside biological tissues can be measured directly by microwave radiometry. This was first proposed by Barrett et al. in the detection of breast cancer [4]. Troyitski [5] and Pasechnik et al. [6] proposed the technique of passive acoustic thermotomography which allows the retrieving of temperature profiles in biological objects up to depths of few centimeters.

The term “thermal tomography” appeared in the 1980s in thermal wave studies initiated by Rosencwaig et al. [7]. In 1983, Busse and Renk suggested measuring defect depth by using a simple geometrical algorithm [8]. Later, Mandelis et al. proposed some algorithms of one- and two-sided thermal wave tomography

based on a 3D diffraction model [9,10] with emphasis on the detection of microscopic defects.

The idea of “dynamic thermal tomography” (DTT) was suggested by Vavilov and Shiryaev in 1985 [11]. A purely geometrical approach, that is characteristic of computed X-ray tomography, is replaced in DTT with the analysis of the evolution of temperature *versus* time. This technique is based on the fact that, in one-sided thermal nondestructive testing (TNDT), deeper material layers are characterized by longer time delays of the thermal response. This is a reflection of the fact that, unlike particles and quanta of electromagnetic radiation, thermal energy propagates in solids by diffusion. DTT allows [12–14] (1) analyzing of solids layer-by-layer, (2) reducing the surface noise which worsens the effectiveness of “classical” TNDT, (3) improving defect “detectability” and (4) evaluating defect depth with a reasonable accuracy (less than 15–20% error).

In this paper, a “reference-free” approach to DTT is proposed being based on some mathematical manipulations with a front-surface temperature response. Also, DTT potentials for processing results of ultrasonic infrared thermography are demonstrated.

## 2. ‘Classical’ DTT

In its original form, the DTT algorithm involves the analysis of the differential temperature signal  $\Delta T(i, j, \tau) = T(i, j, \tau) - T(i_{ref}, j_{ref}, \tau)$ ,

\* Tel.: +7 913 821 9749; fax: +7 3822 417281.

E-mail address: [vavilov@tpu.ru](mailto:vavilov@tpu.ru)

where  $T$  is the specimen excess temperature,  $\tau$  is the time and the subscript “ref” relates to a reference point to be chosen by an operator. In an IR image sequence of an arbitrary length, each pixel  $(i, j)$  can be characterized by the maximum signal  $\Delta T_m(i, j)$  and the time of its appearance  $\tau_{m \leftarrow}(i, j)$ . Such an approach results in synthetic images called, respectively, maxigram and timegram.

The “classical” approach to TNDT is based on solutions to direct 3D heat conduction problems for solid bodies with subsurface flaws subjected to thermal stimulation.

The DTT concept is illustrated in Fig. 1 by analyzing a typical 3D TNDT model. Numerical simulation has been fulfilled by using the ThermoCalc-6L software from Tomsk Polytechnic University [15]. A 2 mm-thick sample made of carbon fiber reinforced plastic (CFRP) composite contains five defects at three depths (0.5, 1 and 1.5 mm) to simulate impact damage. This kind of defects is often undetectable at the impact point but it starts to grow laterally with increasing depth and reaches its maximum size near the rear surface (see the experimental example in p. 6.2). Note that the model includes a local variation in CFRP emissivity  $\varepsilon$  ( $E$ ) from 0.85 to 0.95 ( $\Delta\varepsilon=0.1$ ) on the front surface in order to demonstrate DTT potentials in discriminating defects and surface clutter. The sample is heated with a heat pulse delivering the energy of  $W=10 \text{ kJ/m}^2$  for  $\tau_h=10 \text{ ms}$ . The relationships between model parameters (Fig. 1a), such as defect lateral dimensions  $H_x H_y$ , thickness  $d$  and depth  $l$ , as well as sample thickness  $L$  and the material thermal properties (see the legend to Fig. 1), and surface temperature signals  $\Delta T$  have been discussed in many publications [16–26] to briefly state the following: (1) pulsed and thermal wave test procedures typically provide close results that is the reflection of a general physical principle related to heat conduction in solids, (2) if defects can occur at any depth throughout a specimen, a two-sided test method may be more effective than a one-sided test method; a one-sided test method has difficulty in detecting defects at the far side of a laminate, especially in thick materials, (3) defect depth, as a factor strongly influencing temperature signals, appears in one-sided solutions, and two-sided solutions are mainly affected by defect thickness, (4) lateral dimensions of defects can be evaluated by their visible surface “footprints” with better results being obtained at the so-called earlier observation times, and (5) temperature signals over defects are linearly proportional to absorbed energy, while some other parameters, such as running temperature contrast and observation time, are independent of it.

Characterization of thermal tomograms by the in-depth coordinate is based on  $\tau_m$  vs.  $l$  calibration curves, such as shown in Fig. 1b. Note that  $\tau_m$  is relatively independent of defect thickness  $d$ . In source IR thermograms, it is difficult to separate surface clutter signals (emissivity variation  $\Delta\varepsilon$ ) from real defects by signal amplitude and shape due to significant lateral heat diffusion (Fig. 1c). Also, it is worth remembering that thermal conductivities in a highly anisotropic composite may differ by the order of magnitude that is well noticed by the distortion of surface temperature indications.

The maxigram in Fig. 1d shows subsurface defects at their best observation times no matter at what times  $\Delta T_m$  values occur. Also, the timegram in Fig. 1e reflects the distribution of optimum observation times  $\tau_m$  for defects at different depths. By choosing a particular  $\tau_{m1} - \tau_{m2}$  interval, one can produce a thermal tomogram (Fig. 1f) which shows two defects within the 0.92–1.16 mm layer.

The comparison between  $\Delta T_m$  (maxigram) and  $\tau_m$  (timegram) distributions is of a special interest. Some non-obvious examples are shown in Fig. 2 in application to the detection of composite defects in CFRP. It is seen that time-domain ( $\tau_m$ ) 3D patterns show the real geometry of defects much better than the images of temperature. Two important cases are shown in Fig. 1b and c; the

topology of  $\tau_m$  images looks reversed in regard to the temperature images. Also, it seems that in some cases it is possible to detect a small, deep defect under a larger shallow one.

The pixel values in maxigrams depend strongly on both the defect depth and thickness, while timegrams are strongly influenced by defect depth. The combination of  $\Delta T_m$  and  $\tau_m$  values allows the calculation of both  $l$  and  $d$  values by robust inversion formulas [23,24].

As in “classical” TNDT, which deals with differential temperature signals, a disadvantage of DTT is the necessity to choose a proper reference point. To overcome this shortcoming that is particularly noticeable in the case of strongly uneven heating, a reference point is to be chosen close to an area of interest that is not obviously convenient since *a priori* information is needed.

### 3. Defect lateral size

The evaluation of defect lateral size is another important aspect of defect characterization in both the temperature and time domains. It is well known that surface temperature «footprints» of subsurface defects diffuse in time, therefore, the so-called early detection technique was proposed to evaluate defect shape and lateral size at earlier stages of thermal stimulation [25,26]. This phenomenon is illustrated on air-filled  $10 \times 10 \times 0.05$  and  $5 \times 5 \times 0.05 \text{ mm}^3$  defects in a 2 mm-thick CFRP sample (Fig. 3). The images in Fig. 3a have been calculated at 0.51 and 2.04 s with  $\tau_m=2.04 \text{ s}$  being the optimum observation time for the larger defect. It is clearly seen that, because of the high CFRP thermal diffusivity in the horizontal direction, defect patterns are blurring in time, thus proving the efficiency of early detection. The lateral heat diffusion is also illustrated with the surface spatial profiles in Fig. 3b calculated at three times:  $0.25\tau_m$ ,  $0.5\tau_m$  and  $\tau_m=2.04 \text{ s}$ . A quantitative comparison of lateral heat diffusion phenomenon can be done by introducing the following evident parameter:  $D = T(x=0) - T(x=x_{\text{edg}}) / \Delta T(x=0)$ , where  $x=0$  and  $x_{\text{edg}}$  correspond to the defect center and edge, respectively ( $x_{\text{edg}} = -5; 5 \text{ mm}$  in the case of Fig. 3b). For the  $10 \times 10 \times 0.05 \text{ mm}^3$  defect, the  $D$  values are 0.60 (0.51 s), 0.56 (1.02 s) and 0.50 (2.04 s) and, for the  $5 \times 5 \times 0.05 \text{ mm}^3$  defect, they are, respectively, 0.50 (0.45 s), 0.42 (0.9 s) and 0.31 ( $\tau_m=1.80 \text{ s}$ ). Obviously, the maximum value is  $D=1$  that corresponds to a hypothetical step-wise surface profile with no lateral heat diffusion.

The temperature evolutions in time are presented in Fig. 3c for some surface points. It appears that the more distant is the point from the defect center, the lower is the  $\Delta T_m$  signal and the longer is the  $\tau_m$  time that is well seen in the corresponding maxigrams and timegrams.

It is worth noting that the concept of early detection can be implemented in DTT. For example, timegrams can be produced by calculating an early process time, using the time  $\tau_\gamma$  instead of  $\tau_m$ , where  $\gamma=0.1-1$  yields a relative value  $\Delta T_\gamma / \Delta T_m$ . Spatial profiles of three characteristic times ( $0.25\tau_m$ ,  $0.5\tau_m$  and  $\tau_m$ ) are shown in Fig. 3d compared to the  $\Delta T_m$  profile ( $10 \times 10 \times 0.05 \text{ mm}^3$  defect). It is seen that the distributions of the time-domain parameters are more flat over the defect than the corresponding temperature distribution (this phenomenon is well seen in all timegrams of Fig. 2). The higher time values appearing out of the defect area produce the so-called artifacts that represent faint “footprints” of defects located in layers other than those “sliced” from a timegram; see the spikes in Fig. 1f. To minimize the formation of artifacts, it has been suggested to threshold  $\Delta T_m$  values by 1–5%, using the fact that abnormal  $\tau_m$  values correspond to rather low  $\Delta T_m$  signals. Such a thresholding procedure may significantly improve the performance of thermal tomograms.

Download English Version:

<https://daneshyari.com/en/article/295036>

Download Persian Version:

<https://daneshyari.com/article/295036>

[Daneshyari.com](https://daneshyari.com)